



Isotopic ecology of Hawaiian green sea turtles (*Chelonia mydas*) and reliability of $\delta^{13}\text{C}$, $\delta^{15}\text{N}$, and $\delta^{34}\text{S}$ analyses of unprocessed bone samples for dietary studies

Adriana Velasquez-Vacca^{1,2} · Jeffrey A. Seminoff³ · T. Todd Jones⁴ · George H. Balazs⁵ · Luis Cardona¹

Received: 22 September 2022 / Accepted: 5 May 2023
© The Author(s) 2023

Abstract

This study conducted stable isotope analysis ($\delta^{13}\text{C}$, $\delta^{15}\text{N}$, and $\delta^{34}\text{S}$) on the epidermis and two skeletal elements (rib and squamosal bones) of Hawaiian green turtles (*Chelonia mydas*) and putative diet items obtained from two neritic sites: the Kona/Kohala coast and Oahu. Turtle tissues were collected in 2018–2020 and diet samples in 2018, 2019, and 2021. The effect of body size and sampling locality on individual bulk tissue isotope values was evaluated, and stable isotope mixing models based on $\delta^{13}\text{C}$, $\delta^{15}\text{N}$, and $\delta^{34}\text{S}$ values from those tissues and four groups of food sources were used to reconstruct diet histories of the turtles. Mixing models indicated that green turtles along the Kona/Kohala coast consumed an omnivorous diet, whereas those from Oahu had an herbivorous diet. These diet make-ups are consistent with published gut content analyses. However, mixing models using the stable isotope ratios in rib and squamosal bone failed to yield reasonable diet histories, probably due to inadequacies of the applied trophic discrimination factor (TDF), a key model parameter. These results further establish that stable isotope ratios in the epidermis can be used effectively to study green turtle diet, but also reveal that more validation—and establishment of appropriate TDFs—is needed before bone can be used reliably to assess green turtle diet.

Keywords Trabecular bone · Cortical bone · Mixing models · Trophic discrimination factor · Trophic ecology · Pacific Ocean

Introduction

Green turtles (*Chelonia mydas*) are megaherbivores occurring in coastal ecosystems of tropical and warm temperate regions worldwide (Wallace et al. 2010). Upon departing nesting beaches as hatchlings, green turtles begin an oceanic

juvenile stage during which they forage within the top 100 m of the water column, and are mostly carnivorous, with some omnivorous tendencies (Parker et al. 2011). After settlement in coastal habitats at the ages of 2–7 years old (Reich et al. 2007; Turner Tomaszewicz et al. 2018, 2022a, b), they shift to a plant-dominated diet, often choosing the most prevalent food resources (e.g., seagrasses and/or marine algae) in their resident home ranges (Esteban et al. 2020). Nevertheless, such ontogenic diet shifts are not as strict as presumed in the past, and green turtles in many areas consume omnivorous diets comprised of vegetal and invertebrate foods (Cardona et al. 2010). Furthermore, specimens as large as 70 cm curved carapace length (CCL) can be found in pelagic waters, suggesting that some turtles delay their recruitment to neritic habitats, or move back and forth between both environments (Cardona et al. 2009; Parker et al. 2011). There is also evidence that some green turtles may remain as long-term pelagic foragers, consuming benthic and mid-water prey for much of their lives (Turner Tomaszewicz et al. 2018).

Responsible Editor: L. Avens.

✉ Adriana Velasquez-Vacca
adriana Velasquezvacca@gmail.com

- ¹ IRBio and Department of Evolutionary Biology, University of Barcelona, Barcelona, Spain
- ² Grupo de Ecología de la Universidad del Valle, Cali, Colombia
- ³ NOAA Fisheries, Southwest Fisheries Science Center, La Jolla, CA, USA
- ⁴ NOAA Fisheries, Pacific Islands Fisheries Science Center, Honolulu, HI, USA
- ⁵ Golden Honu Services of Oceania, Honolulu, HI, USA

The Hawaiian Islands support a distinct population of green turtles (Wallace et al. 2010), once seriously depleted but currently experiencing a vigorous rebound (Seminoff et al. 2015; Piacenza et al. 2016). Hawaiian green turtles settle to neritic habitats and transition to a macroalgae-based diet when approximately 40 cm CCL, according to gut content analyses (Arthur and Balazs 2008; Russell and Balazs 2009, 2015). Their diet across the archipelago also includes small amounts of terrestrial vegetation (Russell et al. 2011; McDerimid et al. 2015, 2018) and some animal prey (Russell and Balazs 2009, 2015), as well as seagrasses (*Halophila hawaiiiana* and *Halophila decipens*) in Oahu (Russell et al. 2003; Arthur and Balazs 2008). It is worth noting that green turtles inhabiting sites with moderate human impacts, such as the Kona/Kohala coast on the leeward side of the Island of Hawaii, feed mostly on intertidal native algae, whereas turtles living at sites with substantial anthropogenic disturbance, such as Kāneʻohe Bay in Oahu, rely mostly on exotic macroalgae (Arthur and Balazs 2008; Russell and Balazs 2015), perhaps driven by loss of other marine algivores from overfishing and the ensuing rise in subtidal exotic macroalgae biomass (Wabnitz et al. 2010).

The variability in green turtle diets across the Hawaiian Archipelago coupled with the disparate patterns of human presence raise questions about the original, historic diet of green turtles in Hawaii. This is especially true considering that animals' diets may vary as their populations recover (Hanson et al. 2009; Zenteno et al. 2015a)—as are Hawaiian green turtles—perhaps due to changes in resource availability due to an increase in intraspecific competition and/or changing environmental conditions.

Retrospective dietary analyses are notoriously challenging and typically require stable isotope analysis (SIA) of consumer tissues collected decades or more in the past, such as those housed in museums (Fleming et al. 2016; Choy et al. 2020). However, inferences from isotopic analyses of museum-preserved specimens require some understanding of past isotopic patterns in the environment, as well as knowledge about the time window reflected by the archived tissues (Zenteno et al. 2015b; Braje et al. 2017).

Epidermal tissue is commonly used for SIA-based dietary analyses for sea turtles (Lemons et al. 2011; Gillis et al. 2018; Pagès Barceló et al. 2021), primarily because two key components for such efforts—trophic discrimination factor and tissue isotopic turnover rate—are well established for this tissue type (Seminoff et al. 2006; Jones and Seminoff 2013). However, the epidermis is infrequently preserved in museum specimens, and instead, skeletal elements such as skull and carapace are the most prevalent in museum collections. Although these tissues offer promise for dietary reconstruction from decades or centuries past, further validation for the use of bones in SIA-derived diet analysis is needed.

Despite the potential value for bone to be used in diet reconstruction it is important to note that skeletal components may vary widely in their composition and development patterns (Ehrlich 2010; Lazarus et al. 2020). Skull and rib bones—among the most frequent skeletal elements in museum collections—consist mostly of a thin layer of cortical bone and a thick core of trabecular bone (Arencibia et al. 2006; Jones et al. 2012), the latter of which is constantly remodeled (Castanet and Smirina 1990) and likely integrates dietary information during a relatively brief period prior to death, compared to cortical bone (Skedros et al. 2013; Fahy et al. 2017). Yet despite their value for integrating dietary information, the time span that might be reflected in analyses of such bones is unknown. Moreover, stable isotope discrimination occurs during metabolism, and tissue-specific routing of assimilated nutrients likely occurs, both of which may result in animal tissues having slightly different isotopic values than their diet (DeNiro and Epstein 1978). This disparity is called the trophic discrimination factor (TDF) and may vary across tissues due to differences in tissue-specific metabolism, biochemical composition, and routing pathways (Bearhop et al. 2002). Because of this, TDF should be experimentally determined for each species and tissue under study to facilitate accurate dietary reconstructions using stable isotope mixing models (Phillips et al. 2014; Stock et al. 2018), which are a primary tool implemented for SIA-based diet study. Whereas TDF values have been determined experimentally for the epidermis and the cortical bone of green turtles (Turner Tomaszewicz et al. 2017), nothing is known about the TDF of trabecular bone (Koch et al. 2007; Turner Tomaszewicz et al. 2015). An additional consideration when evaluating bone in stable isotope studies is the influence of lipids and the mineral matrix on the stable isotope values of the consumer and the diet item. This is important because lipids are highly depleted in ^{13}C and hence integrating stable isotope values of tissues with differing lipid and/or collagen:apatite concentrations into isotope mixing models could lead to erroneous dietary reconstructions (Post 2002). To measure the stable isotope ratio of carbon in bone, samples are typically demineralized with such as HCL (Turner Tomaszewicz et al. 2015), and lipids are removed with organic solvents (Bas and Cardona 2018; Bas et al. 2020), yet these treatments have not been universally employed among SIA dietary studies.

Here, we use the $\delta^{13}\text{C}$, $\delta^{15}\text{N}$ and $\delta^{34}\text{S}$ values in the epidermis, squamosal bone, and rib bone of modern Hawaiian green turtles to (1) quantify the effect of lipids and carbonates on isotope values in bone samples to derive an equation to correct for both in unprocessed samples, (2) compare isotope values among the three tissue types, (3) understand the effect of body size and geographic location on the isotope values of modern Hawaiian green turtles, and (4) establish the efficacy of using skeletal elements for

diet analysis by comparing their mixing model results with those of epidermis, which is well-established for SIA dietary reconstruction.

We used an equation calculated with the $\delta^{13}\text{C}$ values of paired unprocessed and processed (to remove lipids and carbonates) green turtle bone samples to assess the effect of lipid extraction and demineralization in bone. Then, we sampled the epidermis, squamosal and rib bones of dead-stranded green turtles in two areas of the main Hawaiian Islands, measured $\delta^{13}\text{C}$, $\delta^{15}\text{N}$ and $\delta^{34}\text{S}$ values in each tissue and assessed the patterns of ontogenetic and geographic variability. Finally, we tested if the TDF values derived from the cortical bone of green turtles (Turner Tomaszewicz et al. 2017) are appropriate to assess the contribution of different sources to the diet of green turtles (Layman et al. 2012; Gillis et al. 2018) using mixing models in squamosal and rib bone.

Materials and methods

Study site

Studies sites were selected to represent two contrasting ecosystems in which passive acoustic- and satellite-tracking have demonstrated prolonged residence of green turtles (Balazs 1976; Balazs and Chaloupka 2004). Oahu supports a diversity of coastal ecosystems including non-native mangrove stands, coral reefs, seagrass meadows and coral rubble fields covered by macroalgae (Allen 1998; McDermid et al. 2007; Williams et al. 2008). This region has a long history of eutrophication driven by human disturbance (Lesser 2021). In contrast, rocky shores with fringing reefs prevail on the oligotrophic and less-disturbed Kona/Kohala coast, on the

Island of Hawaii, (McDermid and Stuercke 2003; Friedlander et al. 2008; Wabnitz et al. 2010; Cardona et al. 2020).

Turtle sample collection and storage

Epidermis and bone samples were taken from 15 dead-stranded green turtles from Oahu and 18 dead-stranded green turtles from the Kona/Kohala coast (Fig. 1). Upon recovery, the dead-stranded green turtles were frozen at $-20\text{ }^\circ\text{C}$. Necropsies were conducted by Pacific Islands Fisheries Science Center (NOAA) staff in Honolulu, Hawaii. During this process, curved carapace length (CCL) was measured and epidermis and bone samples were collected. Epidermis samples (ca. $0.5 \times 0.5\text{ cm}$) were taken from the shoulder region using a razor blade and stored in 2 ml cryovials with a saturated salt solution. Special attention was given to only collect the epidermal layer and no underlying connective tissue. No epidermis samples were collected from turtles in advanced decomposition. In addition, pieces of squamosal and rib bone were cut from each turtle, rinsed with deionized water, air-dried, and stored in Whirl-Pak[®] bags. All samples were transported to Southwest Fisheries Science Center (La Jolla, California, USA) and stored at $-20\text{ }^\circ\text{C}$ until processing.

Diet items sample collection

Previous gut content studies had revealed that the diet of Hawaiian green turtles foraging in the coastal waters off Oahu from 1977 to 2012 was dominated by red macroalgae (*Acanthophora spicifera*, *Gracilaria salicornia*, and *Hypnea musciformis*), with the seagrasses *H. decipens*, and *H. hawaiiiana* supplying less than 15% of the ingested material (Russell et al. 2003; Russell and Balazs 2015). Conversely,

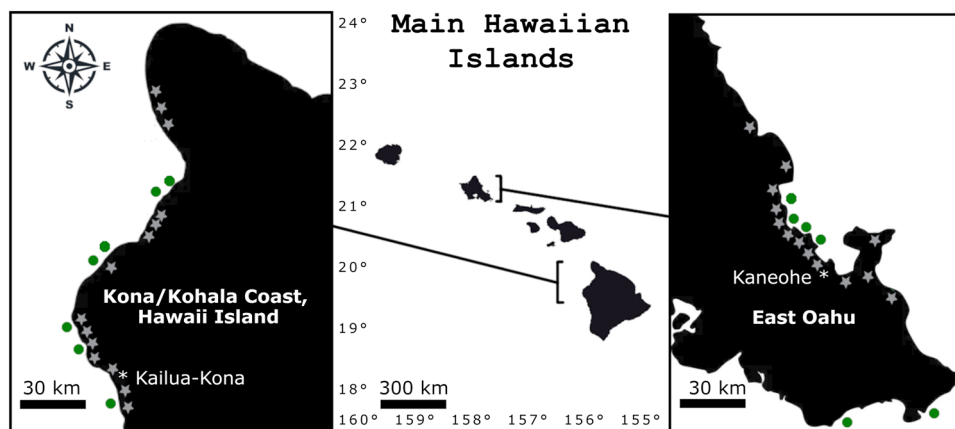


Fig. 1 Sampling locations on Oahu and Kona/Kohala coast, Hawaii. The green circles indicate places where turtles were found dead-stranded. A grey star represents locations for diet items sampling. Diet items sampling locations on Oahu were: Wailupe, Kāneʻohe

flats, Kāneʻohe reef, Kāneʻohe sandbar, Wawamalu; and on the Kona/Kohala coast: Kiholo, Waialea, Kaloko-Honokōhau National Historical, Waialea, Honokōhau Kalaoa small harbor. Maps modified from R tmap (Tennekes 2018)

the diet of green turtles foraging off the Kona/Kohala coast was dominated by red macroalgae in the genus *Pterocladia* (Arthur and Balazs 2008). Hawaiian green turtles also consume lesser amounts of animal prey (Arthur and Balazs 2008; Russell et al. 2011). Those on the Kona/Kohala coast are observed regularly scavenging fish scraps at the Honokōhau Small Boat Harbor (G. Balazs, personal observation). Accordingly, we sampled the macroalgae *A. spicifera*, *G. salicornia*, and *H. musciformis*, the seagrass *H. hawaiiiana*, and turf algae from Oahu, and the macroalgae *G. salicornia*, *H. musciformis*, and *P. capillacea* and turf algae from the Kona/Kohala coast. Turf algae are dense, multi-species assemblages of filamentous benthic algae, including small patches of macroalgae and cyanobacteria, typically less than 1 cm in height (Swierts and Vermeij 2016). Both areas (Oahu and the Kona/Kohala coast) were sampled at the end of the dry (September 2018) and rainy seasons (February 2019). Red mangrove leaves (*Rhizophora mangle*) and scraps of mahi-mahi (*Coryphaena hippurus*) were collected at Wawamalu (Oahu) and Honokōhau Small Boat Harbors (Kona/Kohala coast), respectively, in March 2021.

Tissue preparation and stable isotope analysis

Bone samples were cross-sectioned and then drilled with a Dremel Tool™ with a 0.1-inch drill bit. The collected powder (approximately 50 mg) was dried at 50 °C for 24 h and sent to the Stable Isotope Core Laboratory at Washington State University for bulk tissue isotope analysis. Before analysis, epidermis samples and putative diet item samples were rinsed with deionized water, dried at 50 °C for 24 h, ground to a fine powder, and also sent to Washington State University for SIA.

For carbon and nitrogen isotopic analysis, green turtle skin and bone samples were ground to fine powder, weighed (to ca. 5 mg), and encapsulated in tin cups. Samples were then combusted in an elemental analyzer (ECS 4010, Costech Analytical Valencia, CA), gases separated with a 3 m GC column and analyzed with a continuous-flow isotope ratio mass spectrometer (Delta Plus XP, Thermo Finnigan, Bremen) (Brenna et al. 1997). Isotopic reference materials were interspersed with samples for calibration. The contribution of ¹⁷O was corrected by the IRMS software using the Santrock correction (Santrock et al. 1985). Carbon isotopic results are reported in parts per thousand (‰) relative to VPDB (Vienna Peedee Belemnite) using NBS 19 and L-SVEC as anchor points. Nitrogen isotope ratios are reported in ‰ in relative to N₂ in air.

Sulfur isotopic analysis of Hawaiian green turtle samples was conducted independently. The powder was weighed (10 mg in bone and epidermis and 5 mg in diet items) and encapsulated at the Stable Isotope Core Laboratory at Washington State University. Prepared samples were combusted

with the same elemental analyzer as C and N samples, and SO₂ gases were separated with a 0.8 m GC column (100 °C) and analyzed with a continuous flow isotope ratio mass spectrometer (Delta Plus XP, Thermo Finnigan, Bremen) (Qi and Coplen 2003). The final determination of δ³⁴S was based on the collection of S ions 64 and 66. A dual reactor configuration was used (Fry et al. 2002), with the second reactor full of quartz chips to buffer ¹⁸O contribution to the SO₂. Approximately 5 mg of niobium pentoxide was amended to each sample to improve combustion. No correction for oxygen isotope contribution was made. Four isotopic reference materials were interspersed with samples for calibration (Costech analytical BBOT, Alpha Aesar BaSO₄, Salt Lake Medals Ag₂S, and Acros elemental S). A grizzly bear hair (*Ursus arctos horribilis*) sample from Pullman, WA, where the stable isotopes laboratory is located, was also run with all samples as a blind QC. Isotopic results are expressed in delta (δ) notation relative to VCDT (Vienna-Canyon Diablo Troilite) in parts per thousand (‰).

Calibration for δ¹³C

Hawaiian green sea turtle bone samples were not demineralized with HCl nor treated with organic solvents to remove lipids before the analysis of δ¹³C (Medeiros et al. 2015; Bas and Cardona 2018). Such pre-processing requires larger amounts of sample, which is not an issue with modern specimens but can be a limiting factor when studying rare museum specimens. (Turner Tomaszewicz et al. 2015) Bone samples used for SIA are typically demineralized with HCl, and lipids are removed with organic solvents before the analysis of C and N stable isotope ratios (Bas and Cardona 2018; Bas et al. 2020) to remove lipids (highly depleted in ¹³C compared to protein) and non-collagen proteins, which are more variable in composition and hence in δ¹⁵N values than collagen (Koch et al. 2007; Turner Tomaszewicz et al. 2015). However, acidification modifies the δ³⁴S values (Connolly and Schlacher 2013), and the measurement of δ¹³C, δ¹⁵N, and δ³⁴S requires sub-sampling, hence a larger amount of sample. To correct for the contribution of non-organic components and lipids to δ¹³C values in our samples, we analyzed 94 bone samples of Mediterranean green turtles from the tissue collection at the University of Barcelona and calculated a calibration equation that could be used to correct mathematically the δ¹³C values of our samples based on the C:N ratios (Turner Tomaszewicz et al. 2015). To calculate this equation, the green turtle bone samples from the University of Barcelona were ground to a fine powder with mortar and pestle and split into two subsamples of approximately 20 mg each.

One subsample was processed for carbon-stable isotope analysis without further treatment. The other subsample was treated as follows: first it was demineralized (dml hereafter)

by soaking in 0.5 N HCl for 24 h, rinsed with distilled water, dried again at 50 °C for 24 h, and lipids were removed through sequential rinses with 2:1 chloroform:methanol until the solution was clear (Folch et al. 1957). After lipid extraction, it was dried at 50 °C for 24 h.

Both treated and not treated powdered samples were then weighed (~0.3 mg) in tin capsules at CCiT (Centres Científics i Tecnològics de la Universitat de Barcelona), combusted at 900 °C, gases separated and analyzed in a continuous flow isotope ratio mass spectrometer (Flash 1112 IRMS Delta C Series EA, Thermo Finnigan, Bremen). Isotopic reference materials were interspersed with samples for calibration, and the contribution of ^{17}O was corrected by the IRMS software using the Santrock correction (Santrock et al. 1985). Paired Student *t* tests were run in R version 4.1.1 (2021-08-10) (R Core Team 2021) to analyze if there were differences in the $\delta^{13}\text{C}$ values between paired treated and untreated samples. Then, an equation to assess the effect of the treatment on carbon values versus no treatment was calculated.

Statistical analysis

Pearson correlation coefficients were calculated for the individual values of each stable isotope ratio ($\delta^{13}\text{C}$, $\delta^{15}\text{N}$, and $\delta^{34}\text{S}$) in each tissue (epidermis, squamosal bone, rib bone), separately for each study site, to explore ontogenetic diet changes. Then, generalized linear models were run in IBM SPSS v. 25 to assess if locality (Oahu and Kona/Kohala coast) and tissue type (squamosal, rib, and epidermis separately) had any significant effect on the $\delta^{13}\text{C}$, $\delta^{15}\text{N}$, and $\delta^{34}\text{S}$ values of turtles after accounting for TDF (see below). MixSIAR (Stock et al. 2018) was used in R to run Bayesian mixing models to analyze $\delta^{13}\text{C}$, $\delta^{15}\text{N}$, and $\delta^{34}\text{S}$ in green turtles and their putative diet items, following the MixSIAR model framework, which estimates the proportion contributions of the source (diet items) to the mixture (green turtle). All JAGS models (Just Another Gibbs Sampler) were run at normal configuration (chain length = 100,000, burn = 50,000, thin = 50, chains = 3). The TDF values used were as follows: mean \pm SE = $+1.9 \pm 0.3\%$ for $\delta^{13}\text{C}_{\text{epidermis}}$ and $+4.1 \pm 0.4\%$ for $\delta^{15}\text{N}_{\text{epidermis}}$, $+1.7 \pm 0.6\%$ for $\delta^{13}\text{C}_{\text{bone}}$ and $+5.1 \pm 1.1\%$ for $\delta^{15}\text{N}_{\text{bone}}$, according to Turner Tomaszewicz et al. (2017).

The TDF for $\delta^{34}\text{S}$ was assumed to be 0 (McCutchan et al. 2003).

Results

Calibration for $\delta^{13}\text{C}$

To analyze the stable isotopes from Hawaiian sea turtles without chemical pre-treatment, a calibration equation was derived from a collection of green sea turtles at Universidad de Barcelona. The difference between the $\delta^{13}\text{C}$ values of paired treated and untreated samples was statistically significant (Paired *t* test, $t_{93} = 12.754$, $p < 0.001$) and ranged from 1.6 to 5.7‰ ($X \pm \text{SE} = 4.1 \pm 1.1\%$). The relationship between the $\delta^{13}\text{C}$ values of paired treated and untreated samples was best described ($r^2 = 0.805$, $p < 0.001$) by the following equation:

$$\delta^{13}\text{C}_{\text{dml}} = \delta^{13}\text{C}_{\text{unp}} - 3.658 + (3.372 \times \ln(C : N)_{\text{unp}}) \quad (1)$$

where $\delta^{13}\text{C}_{\text{dml}}$ denotes the $\delta^{13}\text{C}$ value after acidification and lipid extraction, $\delta^{13}\text{C}_{\text{unp}}$ denotes the $\delta^{13}\text{C}$ value in unprocessed samples, and $(C:N)_{\text{unp}}$ is the atomic ratio of unprocessed samples. Accordingly, this equation was used to calibrate the $\delta^{13}\text{C}_{\text{unp}}$ values of all bone samples for green turtles from Hawaii.

Hawaiian green turtle stable isotope values in epidermis and bone tissue

Hawaiian green turtle CCLs ranged 45.1–102.5 cm (mean \pm SE = 72.14 ± 13.45 cm, $n = 15$) at Oahu and 39.0–98.6 cm (mean \pm SE = 53.89 ± 17.45 cm, $n = 18$) at Kona/Kohala coast. Rib and squamosal bone samples were collected from all turtles included in this study. Epidermis samples were missing from 2 turtles from Oahu and from 6 turtles on the Kona/Kohala coast due to severe decomposition. The mean stable isotope ratios of each tissue from green turtles on each island are reported in Table 1, and the results of the Pearson correlation analysis are reported in Table 2. Correlations were calculated for the individual

Table 1 Mean stable isotope ratios values and standard error for squamosal, rib, and epidermis of green turtles from Oahu and Kona/Kohala coast

Study site	Tissue type	<i>n</i>	$\delta^{13}\text{C}$ ‰ (\pm SE)	$\delta^{15}\text{N}$ ‰ (\pm SE)	$\delta^{34}\text{S}$ ‰ (\pm SE)
Oahu	Bone (squamosal)	15	-11.94 ± 1.09	7.46 ± 1.13	14.60 ± 1.16
	Bone (rib)	15	-12.43 ± 1.41	7.96 ± 1.42	15.95 ± 1.13
	Epidermis	13	-13.90 ± 1.61	8.53 ± 1.28	18.15 ± 1.22
Kona coast	Bone (squamosal)	18	-12.29 ± 1.37	9.71 ± 1.14	16.16 ± 1.06
	Bone (rib)	18	-12.29 ± 1.37	9.71 ± 1.14	16.16 ± 1.06
	Epidermis	12	-13.56 ± 1.33	10.05 ± 1.09	17.31 ± 1.27

Carbon ratios were corrected for acidification and lipid extraction (Eq. 1)

Table 2 Pearson correlations between $\delta^{13}\text{C}$, $\delta^{15}\text{N}$, and $\delta^{34}\text{S}$ values in the epidermis, squamosal bone, and rib bone of green turtles from Hawaii

Isotope/tissue combination	r	p	n
$\delta^{13}\text{C}_{\text{sq}} / \delta^{13}\text{C}_{\text{rib}}$	0.09	<0.001	33
$\delta^{13}\text{C}_{\text{sq}} / \delta^{13}\text{C}_{\text{epi}}$	0.54	0.006	25
$\delta^{13}\text{C}_{\text{sq}} / \delta^{15}\text{N}_{\text{sq}}$	0.69	<0.001	33
$\delta^{13}\text{C}_{\text{sib}} / \delta^{13}\text{C}_{\text{epi}}$	0.68	<0.001	25
$\delta^{13}\text{C}_{\text{rib}} / \delta^{15}\text{N}_{\text{rib}}$	0.65	<0.001	33
$\delta^{15}\text{N}_{\text{sq}} / \delta^{15}\text{N}_{\text{rib}}$	0.91	<0.001	33
$\delta^{15}\text{N}_{\text{sq}} / \delta^{15}\text{N}_{\text{epi}}$	0.67	<0.001	25
$\delta^{15}\text{N}_{\text{sq}} / \delta^{34}\text{S}_{\text{sq}}$	0.44	<0.001	33
$\delta^{15}\text{N}_{\text{rib}} / \delta^{15}\text{N}_{\text{epi}}$	0.63	<0.001	25
$\delta^{15}\text{N}_{\text{sq}} / \delta^{15}\text{N}_{\text{rib}}$	0.47	0.015	25

Only significant correlations between the stable isotope ratios of the same element across tissues or different elements within the same tissue are shown

rib Rib bone, *sq* squamosal bone, *epi* epidermis

values of each stable isotope ratio in each tissue, separately for each study site. The $\delta^{13}\text{C}$ and $\delta^{15}\text{N}$ values were negatively correlated, and $\delta^{13}\text{C}$ and $\delta^{34}\text{S}$ values were uncorrelated, in the three tissues when all turtles were considered. However, $\delta^{15}\text{N}$ and $\delta^{34}\text{S}$ values were positively correlated in the squamosal bone but uncorrelated in the epidermis and the rib bone (Table 2).

No significant difference was found between the $\delta^{13}\text{C}$ values of green turtles from Oahu (mean \pm SE = $-11.94 \pm 1.19\text{‰}$ in squamosal, mean \pm SE = $-12.43 \pm 1.99\text{‰}$ in rib, mean \pm SE = $-13.90 \pm 2.60\text{‰}$ in epidermis) and Kona/Kohala coast (mean \pm SE = $-12.29 \pm 1.90\text{‰}$ in squamosal, mean \pm SE = $-11.92 \pm 2.09\text{‰}$ in rib, mean \pm SE = $-13.56 \pm 1.77\text{‰}$ in epidermis) (Fig. 2) for any of the three tissues or between the $\delta^{13}\text{C}$ values of squamosal and rib bone, although epidermis was significantly depleted in ^{13}C compared to bone [GLM, $F(5,92) = 3.048$, $p = 0.014$] tissue [GLM, $F(2,92) = 6.985$, $p < 0.002$], island [GLM, $F(1,92) = 0.305$, $p = 0.582$] and their interaction [GLM, $F(2,92) = 0.415$, $p = 0.662$]. The three tissues were significantly more enriched in ^{15}N in green turtles from Kona/Kohala coast (mean \pm SE = $9.71 \pm 1.32\text{‰}$ in squamosal, mean \pm SE = $9.42 \pm 1.47\text{‰}$ in rib, mean \pm SE = $10.05 \pm 1.19\text{‰}$ in epidermis) relative to those from Oahu (mean \pm SE = $8.53 \pm 1.64\text{‰}$ in the skin, mean \pm SE = $7.46 \pm 1.29\text{‰}$ in squamosal, mean \pm SE = $7.96 \pm 2.04\text{‰}$ in rib), and no significant differences were found among the $\delta^{15}\text{N}$ values for the three tissues from green turtles within each area [GLM, $F(5,92) = 5.146$, $p < 0.001$], tissue [GLM, $F(2,92) = 1.073$, $p = 0.346$], island [GLM, $F(1,92) = 23.508$, $p < 0.001$] and interaction [GLM, $F(2,92) = 0.198$, $p = 0.820$]. Finally, $\delta^{34}\text{S}$

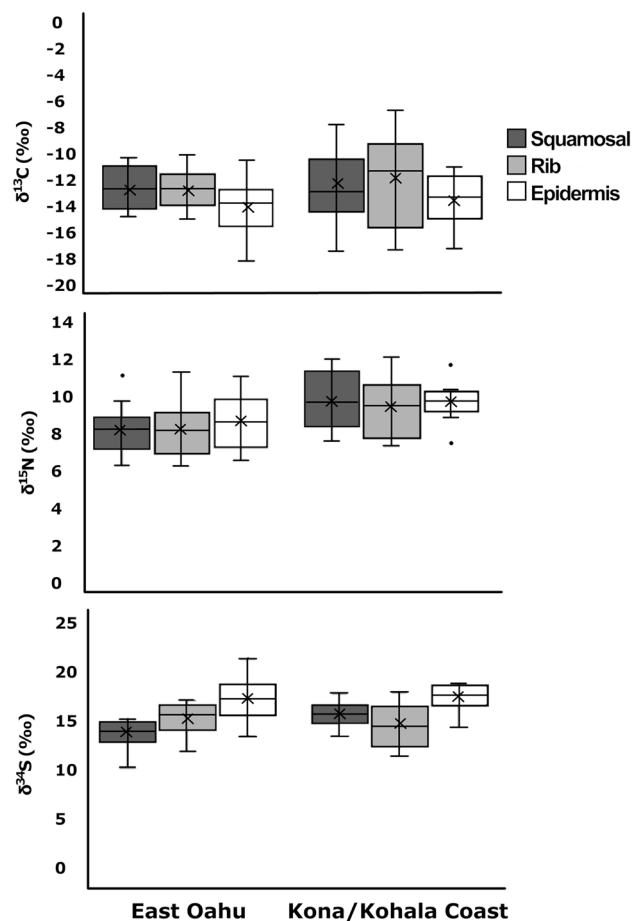


Fig. 2 Stable isotope ratios of carbon, nitrogen and sulfur in squamosal, rib, and epidermis samples from the green turtle on Oahu and Kona/Kohala coast. The whiskers represent the minimum and maximum values, and the dots are the outliers. The mean is shown as an x, and the median as a line: the box represents the interquartile range (the bottom line of the box represents the median of the bottom half or 1st quartile, and the top line of the box represents the median of the top half or 3rd quartile)

values did not differ between green turtles at the two islands for any tissue (mean \pm SE = 14.60 ± 1.36 in squamosal, mean \pm SE = 15.95 ± 1.29 in rib, mean \pm SE = 18.15 ± 1.49 in epidermis in Oahu and mean \pm SE = $16.16 \pm 1.14\text{‰}$ in squamosal, mean \pm SE = $15.13 \pm 1.78\text{‰}$ in rib, mean \pm SE = $17.31 \pm 1.63\text{‰}$ in epidermis in the Kona/Kohala coast). The epidermis was significantly enriched in ^{34}S compared to squamosal and rib bone. However, the tissue and island interaction was significant because the average $\delta^{34}\text{S}$ value of the squamosal of the green turtles from Oahu was lower than that of the Kona/Kohala coast. No difference existed between the average $\delta^{34}\text{S}$ value of the two areas for rib or epidermis [GLM, $F(5,92) = 8.700$, $p < 0.001$], tissue [GLM, $F(5,92) = 15.882$, $p < 0.001$], island [GLM, $F(1,92) = 1.257$, $p = 0.265$], interaction [GLM, $F(5,92) = 5.718$, $p = 0.005$].

Table 3 Pearson correlations between turtle size (CCL), the stable isotope ratios of $\delta^{13}\text{C}$, $\delta^{15}\text{N}$, and $\delta^{34}\text{S}$ values in the squamosal bone (sq), rib bone (rib), and epidermis (epi) of green turtles from Oahu and the Kona/Kohala coast

Location	Compared pair	<i>r</i>	<i>p</i>	<i>n</i>
Oahu	CCL- $\delta^{34}\text{S}_{\text{rib}}$	0.73	0.003	14
	$\delta^{13}\text{C}_{\text{sq}}/\delta^{13}\text{C}_{\text{rib}}$	0.81	<0.001	15
	$\delta^{13}\text{C}_{\text{sq}}/\delta^{15}\text{N}_{\text{sq}}$	0.72	0.002	15
	$\delta^{13}\text{C}_{\text{sq}}/\delta^{15}\text{N}_{\text{rib}}$	0.74	0.002	15
	$\delta^{13}\text{C}_{\text{rib}}/\delta^{15}\text{N}_{\text{sq}}$	0.78	<0.001	15
	$\delta^{13}\text{C}_{\text{rib}}/\delta^{15}\text{N}_{\text{rib}}$	0.84	<0.001	17
	$\delta^{13}\text{C}_{\text{epi}}/\delta^{15}\text{N}_{\text{tpi}}$	0.78	0.002	13
	$\delta^{15}\text{N}_{\text{sq}}/\delta^{15}\text{N}_{\text{rib}}$	0.92	<0.001	15
	$\delta^{15}\text{N}_{\text{sq}}/\delta^{15}\text{N}_{\text{epi}}$	0.63	0.020	13
	$\delta^{15}\text{N}_{\text{rib}}/\delta^{15}\text{N}_{\text{epi}}$	0.63	<0.001	25
	$\delta^{15}\text{N}_{\text{rib}}/\delta^{15}\text{N}_{\text{epi}}$	0.66	0.015	13
Kona/Kohala coast	CCL- $\delta^{15}\text{N}_{\text{sq}}$	0.66	0.027	11
	CCL- $\delta^{15}\text{N}_{\text{rib}}$	0.59	0.016	16
	CCL- $\delta^{34}\text{S}_{\text{sq}}$	0.66	0.029	11
	$\delta^{13}\text{C}_{\text{sq}}/\delta^{13}\text{C}_{\text{epi}}$	0.98	<0.001	18
	$\delta^{13}\text{C}_{\text{sq}}/\delta^{15}\text{N}_{\text{sq}}$	0.70	<0.001	12
	$\delta^{13}\text{C}_{\text{sq}}/\delta^{15}\text{N}_{\text{rib}}$	-0.83	<0.001	18
	$\delta^{13}\text{C}_{\text{sq}}/\delta^{15}\text{N}_{\text{epi}}$	0.72	0.008	12
	$\delta^{13}\text{C}_{\text{rib}}/\delta^{15}\text{N}_{\text{sq}}$	-0.83	<0.001	18
	$\delta^{13}\text{C}_{\text{rib}}/\delta^{15}\text{N}_{\text{rib}}$	-0.78	<0.001	18
	$\delta^{13}\text{C}_{\text{epi}}/\delta^{15}\text{N}_{\text{rib}}$	-0.82	<0.001	12
	$\delta^{13}\text{C}_{\text{epi}}/\delta^{15}\text{N}_{\text{epi}}$	-0.82	<0.001	12
$\delta^{13}\text{C}_{\text{epi}}/\delta^{15}\text{N}_{\text{sq}}$	-0.67	0.017	12	
$\delta^{15}\text{N}_{\text{sq}}/\delta^{15}\text{N}_{\text{epi}}$	0.89	<0.001	18	

Only significant correlations are shown

Relationships between size and isotope value

The curved carapace length (CCL) of the green turtles from Oahu was uncorrelated to $\delta^{13}\text{C}$ and $\delta^{15}\text{N}$ values for all tissues, but it was negatively correlated to the $\delta^{34}\text{S}$ in the rib (Table 3). The correlation between CCL and $\delta^{34}\text{S}$ in the squamosal approached significance (Pearson, $r_{13} = -0.54$, $p = 0.059$). Conversely, the CCL of green turtles from the Kona/Kohala coast was positively correlated with $\delta^{13}\text{C}$ values of the epidermis, but the correlation was not significant for the $\delta^{13}\text{C}$ values of squamosal (Pearson, $r_{16} = 0.46$, $p = 0.076$) and rib (Pearson, $r_{13} = 0.48$, $p = 0.063$). Size (CCL) was negatively correlated to the $\delta^{15}\text{N}$ value of squamosal and epidermis but was not significant for rib (Pearson, $r_{16} = -0.47$, $p = 0.064$). Finally, CCL was uncorrelated to the $\delta^{34}\text{S}$ values of all tissues.

Stable isotope values of diet items

The four diet groups from Oahu included red mangrove leaves, seagrass (*H. hawaiiiana*), macroalgae, and turf. Red mangrove leaves had the lowest $\delta^{13}\text{C}$ and $\delta^{34}\text{S}$ values and the highest $\delta^{15}\text{N}$ values of the considered potential diet items (Figs. 3 and 4). *Halophila hawaiiiana* had the highest $\delta^{13}\text{C}$ values, the lowest $\delta^{15}\text{N}$ values, and intermediate $\delta^{34}\text{S}$ values. Macroalgae (*A. spicifera*, *G. salicornia*, and *H. musciformis*) and turf had $\delta^{13}\text{C}$ and $\delta^{15}\text{N}$ values intermediate between those of red mangrove leaves and *H. hawaiiiana* and higher $\delta^{34}\text{S}$ values than any of them. Turf was more enriched in ^{15}N than macroalgae and hence was included in a group different from macroalgae.

Fig. 3 Isospace for $\delta^{13}\text{C}$ and $\delta^{15}\text{N}$ values in green turtle bone (squamosal and rib) and epidermis on Oahu and Kona/Kohala coast after correcting for the TDF (trophic discrimination factor). The TDF values were as follows: mean \pm SE = $+1.9 \pm 0.3\text{‰}$ for $\delta^{13}\text{C}$ and $+4.1 \pm 0.4\text{‰}$ for $\delta^{15}\text{N}$ in the skin, and $+1.7 \pm 0.6\text{‰}$ for $\delta^{13}\text{C}$ and $+5.1 \pm 1.1\text{‰}$ for $\delta^{15}\text{N}$ in bone, according to Turner Tomaszewicz et al. (2017). Black dots represent each turtle specimen and color dots and lines are the mean and standard deviation of the diet item of the same color

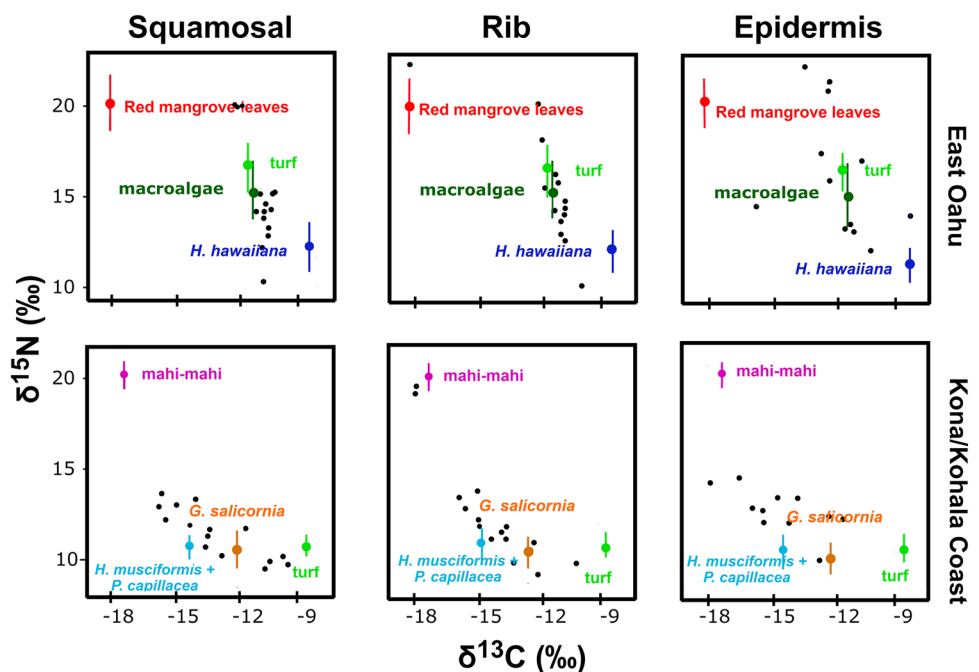
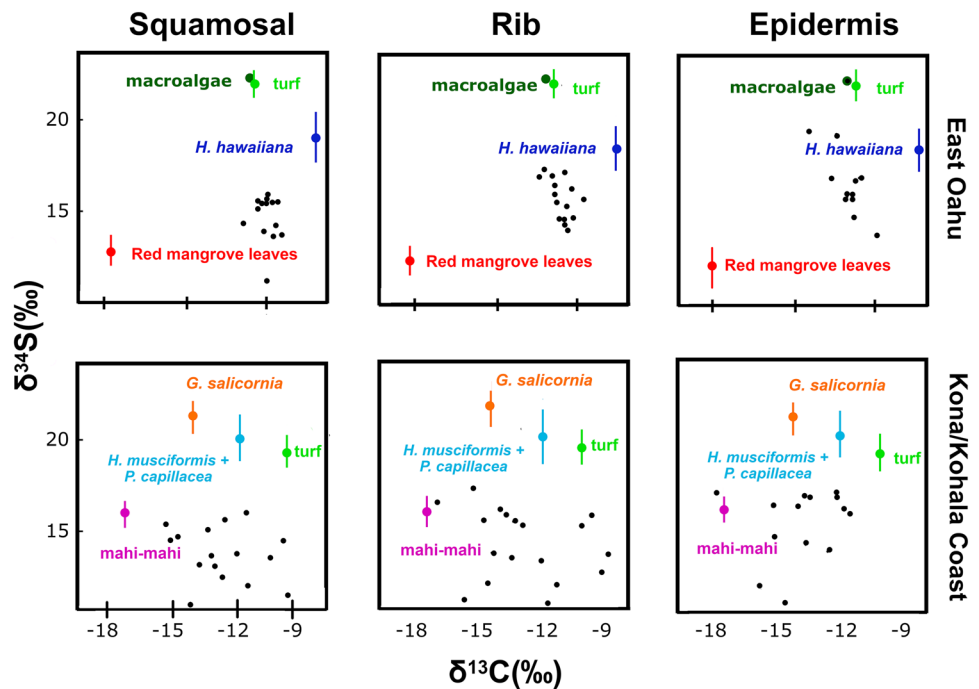


Fig. 4 Isospace for $\delta^{13}\text{C}$ and $\delta^{34}\text{S}$ values in green turtle bone (squamosal and rib) and epidermis on Oahu and Kona/Kohala coast after correcting for the TDF (trophic discrimination factor). The TDF values were as follows: mean \pm SE = $+1.9 \pm 0.3\text{‰}$ for $\delta^{13}\text{C}$ in the skin, and $+1.7 \pm 0.6\text{‰}$ in bone, according to Turner Tomaszewicz et al. (2017). The TDF for $\delta^{34}\text{S}$ was assumed to be 0 (McCutchan et al. 2003). Black dots represent each turtle specimen and color dots and lines are the mean and standard deviation of the diet item of the same color



The four groups from Kona/Kohala included *Gracilaria*, *Hypnea-Pterocladia*, Mahi-Mahi, and turf. They also differed in their $\delta^{13}\text{C}$, $\delta^{15}\text{N}$, and $\delta^{34}\text{S}$ values (Table 2). Mahi-mahi was the most isotopically distinct diet item and was characterized by high $\delta^{15}\text{N}$ values and low $\delta^{13}\text{C}$ and $\delta^{34}\text{S}$. Algae and turf differed in $\delta^{13}\text{C}$ values but not in $\delta^{15}\text{N}$ or $\delta^{34}\text{S}$ values. Among potential diet items, *G. salicornia* was more enriched in ^{13}C than any other, and turf was more enriched in ^{13}C than *H. musciformis* or *P. capillacea* (Fig. 2). The latter two were pooled for statistical analysis and MixSIAR models.

Mixing model results

Most of the squamosal, rib, and epidermis samples from Oahu laid within the mixing polygon formed by turf, macroalgae, and *H. hawaiiiana* in the $\delta^{13}\text{C}$ – $\delta^{15}\text{N}$ isospace after correcting for the TDF (Fig. 3). However, $\delta^{34}\text{S}$ values in those three tissues were much lower than those of the three sources mentioned (Figs. 4 and 5) if TDF = 0. Only when red mangrove leaves were considered a potential food source did all the squamosal, rib, and epidermis samples from Oahu lay within the mixing polygon. Hence, MixSIAR estimated that red mangrove leaves contributed approximately 15% to the assimilated diet of green turtles on Oahu, independently of the tissue considered (Table 4). However, MixSIAR estimated disparate contributions of the remaining diet item groups to the diet of green turtles from Oahu depending on the tissue considered. According to $\delta^{13}\text{C}$, $\delta^{15}\text{N}$, and $\delta^{34}\text{S}$ mixing model analyses for the

epidermis, macroalgae dominated the diet of green turtles (mean \pm SE = $42.1 \pm 33.5\%$), followed by *H. hawaiiiana* (mean \pm SE = $29.3 \pm 27.6\%$). However, credible intervals were loose for both. Conversely, $\delta^{13}\text{C}$, $\delta^{15}\text{N}$, and $\delta^{34}\text{S}$ values in bone, both squamosal and rib, identified *H. hawaiiiana* as the main dietary source (rib: mean \pm SE = $74.8 \pm 6.7\%$, squamosal: mean \pm SE = $73.4 \pm 8.2\%$) and indicated a much lower contribution for macroalgae (rib: mean \pm SE = $3.8 \pm 7.0\%$, squamosal: mean \pm SE = $5.8 \pm 8.7\%$).

Several samples of the epidermis, squamosal, and rib bone from the Kona/Kohala coast laid outside the mixing polygon formed by turf and the three species of macroalgae in the $\delta^{13}\text{C}$ – $\delta^{15}\text{N}$ isospace, because they were highly depleted in ^{13}C and enriched in ^{15}N (Fig. 3). Only when mahi-mahi was included as a potential source did all the samples lay within the mixing polygon. However, some of the squamosal, rib, and epidermis samples from the Kona/Kohala coast were depleted in ^{34}S compared to macroalgae, turf, and mahi-mahi. They laid outside the mixing polygons formed by those four sources in the $\delta^{13}\text{C}$ – $\delta^{34}\text{S}$ (Fig. 4) and the $\delta^{15}\text{N}$ – $\delta^{34}\text{S}$ (Fig. 5) isospaces. This highlights the importance of having at least three different isotopes that show if diet items are missing from the diet composition. According to MixSIAR results, *H. musciformis*–*P. capillacea* was the primary source of assimilated nutrients for the green turtles inhabiting the Kona/Kohala coast when using both squamosal (X \pm SE = $47.9 \pm 18.3\%$) and epidermis samples (mean \pm SE = $54.2 \pm 19.4\%$). Turf was the secondary source (squamosal: mean \pm SE = $31.1 \pm 22.2\%$, epidermis: mean \pm SE = $22.8 \pm 20.7\%$).

Fig. 5 Isospace for $\delta^{15}\text{N}$ and $\delta^{34}\text{S}$ values in green turtle bone (squamosal and rib) and epidermis on Oahu and Kona/Kohala coast after correcting for the TDF (trophic discrimination factor). The TDF values were as follows: mean \pm SE = $+4.1 \pm 0.4\text{‰}$ for $\delta^{15}\text{N}$ in the skin and $+5.1 \pm 1.1\text{‰}$ in bone, according to Turner Tomaszewicz et al. (2017). The TDF for $\delta^{34}\text{S}$ was assumed to be 0 (McCutchan et al. 2003). Black dots represent each turtle specimen and color dots and lines are the mean and standard deviation of the diet item of the same color

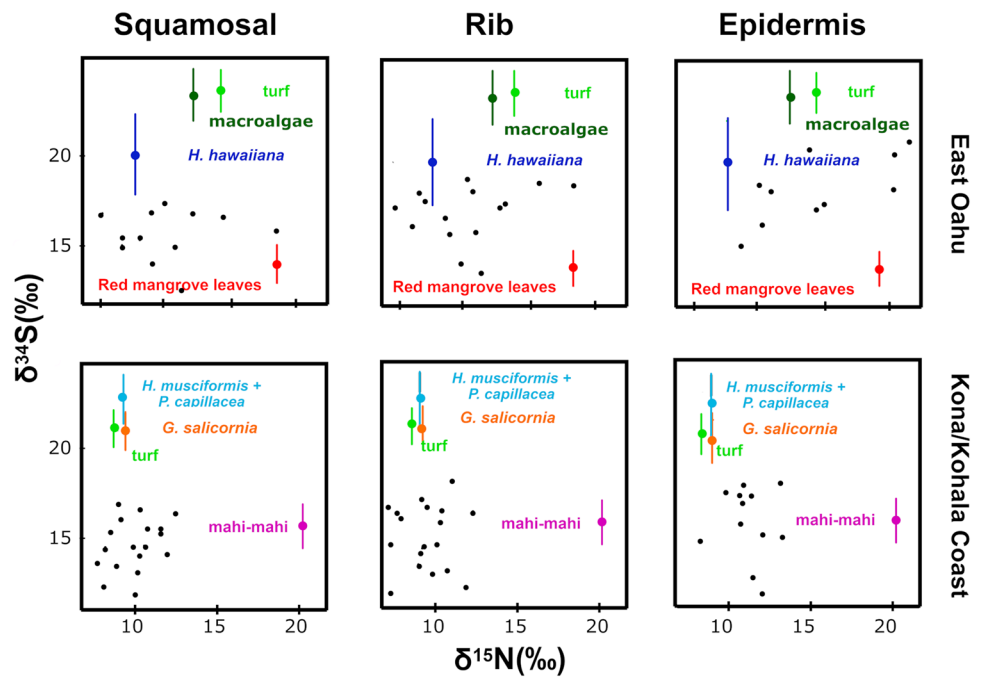


Table 4 Diet items contribution to green turtle diet from the squamosal, rib, and epidermis tissue on Oahu and Kona/Kohala coast estimated using MixSIAR

Tissue	Diet item	Mean diet contribution	Stdv	5.0%	95.0%
Winward Oahu					
Bone (rib)	<i>Halophila</i> spp.	0.75	0.07	0.61	0.80
	Macroalgae	0.04	0.07	0.00	0.17
	Red mangrove leaves	0.20	0.03	0.15	0.23
	Turf	0.02	0.03	0.00	0.07
Epidermis	<i>Halophila</i> spp.	0.29	0.28	0.02	0.71
	Macroalgae	0.42	0.34	0.01	0.85
	Red mangrove leaves	0.13	0.10	0.03	0.28
	Turf	0.16	0.23	0.00	0.73
Bone (squamosal)	<i>Halophila</i> spp.	0.73	0.08	0.56	0.80
	Macroalgae	0.06	0.09	0.00	0.25
	Red mangrove leaves	0.18	0.03	0.12	0.21
	Turf	0.03	0.05	0.00	0.12
Kona/Kohala coast					
Bone (rib)	<i>Gracilaria salicornia</i>	0.15	0.10	0.01	0.34
	<i>Hypnea-Pterocladia</i>	0.34	0.22	0.02	0.70
	<i>Coryphaena hippurus</i>	0.04	0.02	0.01	0.09
	Turf	0.47	0.27	0.04	0.86
Epidermis	<i>Gracilaria salicornia</i>	0.05	0.04	0.01	0.14
	<i>Hypnea-Pterocladia</i>	0.54	0.19	0.07	0.76
	<i>Coryphaena hippurus</i>	0.18	0.03	0.12	0.23
	Turf	0.23	0.21	0.03	0.73
Bone (squamosal)	<i>Gracilaria salicornia</i>	0.15	0.09	0.02	0.31
	<i>Hypnea-Pterocladia</i>	0.48	0.18	0.12	0.74
	<i>Coryphaena hippurus</i>	0.06	0.03	0.02	0.11
	Turf	0.31	0.22	0.02	0.73

Stable isotope ratios in ribs also showed a high contribution of *H. musciformis*—*P. capillacea* to the green turtle diet (mean \pm SE = $34.2 \pm 22.1\%$), but only second most important relative to turf (mean \pm SE = $46.5 \pm 27.4\%$). Nevertheless, discriminating between the actual contribution of *H. musciformis*—*P. capillacea* and turf to the diet of green turtles is difficult considering the loose credible intervals. In any case, the stable isotope ratios in the three tissues suggest a minor role for *G. salicornia* and Mahi-mahi (Table 4).

Discussion

This analysis of the stable isotope ratios of three chemical elements in three different tissues of modern Hawaiian green turtles offers new insight into the trophic ecology of the species and supports the possibility of conducting retrospective studies using the skeletal elements preserved at museums. To this aim, an equation has been calculated for the calibration of carbon stable isotope values in green sea turtle bone, which minimizes the amount of bone powder necessary for the study of rare museum specimens.

Results revealed differences in the $\delta^{13}\text{C}$, $\delta^{15}\text{N}$, and $\delta^{34}\text{S}$ values of the epidermis compared to the two skeletal elements of green turtles (squamosal and rib), but no differences between the two skeletal elements (Fig. 2). Furthermore, body size and sampling locality had similar effects on the stable isotope ratios of squamosal, rib, and epidermis, although the effect was stronger for epidermis. These results revealed differences in the isotopic values of green turtles from Oahu vs. turtles from the Kona/Kohala coast. Additionally, mixing models based on the $\delta^{13}\text{C}$, $\delta^{15}\text{N}$, and $\delta^{34}\text{S}$ values of epidermis indicated a diet make-up similar to that inferred from prior stomach content analysis, hence confirming the reliance of Hawaiian green turtles on macroalgae. In contrast, the output of mixing models based on bone $\delta^{13}\text{C}$, $\delta^{15}\text{N}$, and $\delta^{34}\text{S}$ values often yielded dietary combinations that did not match previous studies, thus suggesting that the $\delta^{13}\text{C}$, $\delta^{15}\text{N}$, and $\delta^{34}\text{S}$ values in the squamosal and rib of green turtles from neritic habitats are informative of diet prior to death, similar to the epidermis, but the TDF of cortical bone derived from the humerus (Turner Tomaszewicz et al. 2017) is not adequate for samples consisting mostly of trabecular bone (squamosal and rib in this study).

Gut content analysis indicates that settlement to neritic habitats and transition to a plant-based diet happen in Hawaiian green turtles at approximately 40 cm CCL, although larger turtles may still consume some animal prey (Russell and Balazs 2009, 2015). The epidermis integrates diet over a few months (Reich et al. 2008), and hence the $\delta^{13}\text{C}$ and $\delta^{15}\text{N}$ values of the epidermis should be uncorrelated to turtle size if the ontogenetic diet shift was abrupt and only neritic individuals were considered; the exception being those rare

turtles sampled or stranded very soon after arrival, which likely represents only a tiny fraction of the population. This is the pattern observed on Oahu but not on the Kona/Kohala coast, where $\delta^{13}\text{C}$ values increase and $\delta^{15}\text{N}$ values decrease as carapace length increases, thus suggesting a more gradual ontogenetic dietary shift in the latter locality. Notably, the same patterns were found when analyzing the epidermis, squamosal, or rib bone.

Previous research has suggested that the pace and timing of the ontogenetic diet shift in green turtles are highly dependent on the relative availability of animal and plant food sources (Cardona et al. 2009; González Carman et al. 2014), and this might be the case for the localities considered here. Oahu supports meadows of *H. hawaiiiana* and *H. decipens* (McDermid et al. 2002; McDermid and Stuercke 2003), extensive red mangrove areas (Allen 1998), and areas of coral rubble with high algal coverage (Cheroske et al. 2000), where green turtles are the most abundant large herbivores (Cardona et al. 2020). Algal availability was even higher in the recent past when the area suffered a high nutrient load (Drupp et al. 2011; Lesser 2021). Conversely, subtidal algal coverage is low along most of the Kona/Kohala coast (Cardona et al. 2020), where sea urchins (mainly *Echinometra mathaei*) and several species of surgeon (Acanthuridae) and parrot fish (Scaridae) are the prevailing subtidal herbivores (Wabnitz et al. 2010; Cardona et al. 2020), and green turtles forage mostly on intertidal turf and macroalgae (Wabnitz et al. 2010). Green turtles inhabiting the Kona/Kohala coast also have access to the fish discarded by anglers at Honokōhau Small Boat Harbor (G. Balazs, personal observation) and fish flesh has also been reported in the gut contents of some green turtles dead-stranded along the Kona/Kohala coast (Russell et al. 2011). Regular fish consumption may explain the high $\delta^{15}\text{N}$ values observed in the epidermis, squamosal, and rib bone of the green turtles from the Kona/Kohala coast compared to those from Oahu. However, the negative correlation between $\delta^{15}\text{N}$ and carapace length suggests declining fish consumption with body size. The same negative correlation is found when analyzing the epidermis, squamosal, and rib bone (Table 3).

Compared to $\delta^{13}\text{C}$ and $\delta^{15}\text{N}$ values, the patterns of variability in the $\delta^{34}\text{S}$ values of the three tissues were harder to interpret, but the inclusion of this third element provided relevant new information (Figs. 1, 2 and 3). Marine primary producers relying only on marine sulfate as a sulfur source are expected to be highly enriched in ^{34}S , whereas those using sulfides formed by bacterial activity in reduced sediments are expected to be depleted in ^{34}S (Fry and Smith 2002; Connolly et al. 2004). The results reported here support this marine-terrestrial gradient, as macroalgae and turf algae from both study areas were enriched in ^{34}S compared to the seagrass *H. hawaiiiana* from Oahu, which in turn was enriched in ^{34}S compared to red mangrove leaves from the

same area. Terrestrial vegetation, which green turtles sometimes consume in Hawaii, according to gut contents analysis and observations (Russell et al. 2011; McDermid et al. 2018), is also depleted in ^{34}S (Rodrigues et al. 2011).

Previous gut content analyses identified the red macroalgae *A. spicifera*, *Gracilaria* spp., and *H. musciformis* as the primary food source of green turtles on Oahu, where *Halophila* seagrasses were the second most important diet item (Russell and Balazs 2015). Similarly, the diet of green turtles on the Kona/Kohala coast has been found to be dominated by red macroalgae in the genera *Pterocladia* and *Hypnea*, followed by *G. salicornia* (Arthur and Balazs 2008). Green turtles have also been observed regularly scavenging fish scraps at the Honokōhau Small Boat Harbor (G. Balazs, personal observation). However, the $\delta^{34}\text{S}$ values of the analyzed diet item in all those sources are too high to explain the $\delta^{34}\text{S}$ values of many of the squamosal and rib bone samples and some skin samples (Figs. 2 and 3). At least one additional yet unsampled ^{34}S -depleted source is likely being consumed by green turtles, particularly on Oahu.

At first glance, red mangrove leaves are a convenient and accessible ^{34}S -depleted source for green turtles on Oahu because they are abundant and are consumed by green turtles elsewhere (Limpus and Limpus 2000; Amorochó and Reina 2007; Nagaoka et al. 2012).

According to MixSIAR, red mangrove leaves might contribute 13% to the diet of green turtles on Oahu, although this consumption has not been reported previously for green turtles in Hawaii. Alternatively, leaves of unidentified terrestrial grasses often occur in the gut contents of green turtles from Oahu (Russell et al. 2011) and might be the primary ^{34}S -depleted source. Similarly, senescent leaves of *Heliotropium foertherianum* are consumed by green turtles along the Kona/Kohala coast (McDermid et al. 2018), thus offering a ^{34}S -depleted source in a region where *Halophila* seagrasses are scarce and occur only deeper than 20 m (McDermid et al. 2002; Russell et al. 2003). In Kona/Kohala, red mangroves were always scarce and have recently been eradicated, so they are probably not the ^{34}S -depleted food source for turtles in this location (Allen 1998) (G. Balazs, personal observation). Further research is necessary to identify the ^{34}S -depleted diet item consumed by green turtles at each locality. However, it is still relevant to note here that analyzing the stable isotopes of sulfur has shed new light on the potential role of red mangroves and terrestrial vegetation in the diet of Hawaiian green turtles.

Despite the uncertainty about the actual identity of the ^{34}S -depleted diet item consumed by green turtles at each locality, results revealed that mixing models combining the $\delta^{13}\text{C}$, $\delta^{15}\text{N}$, and $\delta^{34}\text{S}$ values of the epidermis using the TDF derived experimentally for green turtle epidermis adequately reflected the gross composition of green turtle diet, as described above. Conversely, mixing models showed a

different result than expected when the $\delta^{13}\text{C}$, $\delta^{15}\text{N}$, and $\delta^{34}\text{S}$ values of rib and squamosal bone were combined with the TDF derived experimentally for cortical bone. This is likely because cortical and trabecular bone metabolism differences result in different TDF values. It should also be noted that all the turtles from Kona/Kohala coast laying outside the mixing polygon delimited by macroalgae and turf were smaller than 47 cm CCL, so they could have been eating a carnivorous diet.

The $\delta^{13}\text{C}$ and $\delta^{15}\text{N}$ values vary across the skeletal elements of several mammals (Clark et al. 2017; Bas et al. 2020; Smith et al. 2020) and fish species (Bas and Cardona 2018) because of differences in assimilation pathways, the turnover rate, and the degree of bone remodeling of their skeletal elements. The relative contribution of cortical and trabecular bone to the structure of the elemental isotope considered (Fahy et al. 2017; Bas et al. 2020) and regional heterothermy (Bas et al. 2020; Smith et al. 2020) explain such variability in mammals. The skeletal elements of sea turtles have a structure like that of mammals (Bjørndal et al. 2003; Snover et al. 2011), and green turtles may also exhibit regional endothermy (Standora et al. 1982), so differences in the stable isotope ratios of $\delta^{13}\text{C}$ and $\delta^{15}\text{N}$ might also vary across their skeletal elements. However, no differences were observed between squamosal and rib bone (Fig. 2), probably because both belong to core areas along the body's central axis and have similar anatomic structures, endothermal dynamics, and likely similar turnover rates.

Conversely, the humerus bone, the focus of most of the previous research on the skeletal elements of sea turtles, is a component of the axial skeleton and has a thick layer of cortical bone (Jones et al. 2012; Medeiros et al. 2015). The cortical layer of the humerus bone has been used to estimate TDF values for green turtle bone (Turner Tomaszewicz et al. 2017), which certainly has a much slower isotope turnover rate than the trabecular bone (Castanet and Smirina 1990). Given this, it was expected that the cortical and trabecular bone of green turtles would differ in their TDF values (Medeiros et al. 2015), which may explain why MixSIAR results differ from the gut content analysis from previous studies (Russell et al. 2003; Russell and Balazs 2015) in the two study areas when using the $\delta^{13}\text{C}$, $\delta^{15}\text{N}$, and $\delta^{34}\text{S}$ values in the squamosal and rib bone. In contrast, MixSIAR using the $\delta^{13}\text{C}$, $\delta^{15}\text{N}$, and $\delta^{34}\text{S}$ values in the epidermis of green turtles and the TDF derived experimentally for the same tissue identified the main diet sources of green turtles in both areas, according to gut content analysis (Russell et al. 2003; Russell and Balazs 2015). This highlights the need for further research on the TDF of trabecular bone before the stable isotope ratios in skeletal elements with a prevalence of this tissue can be used for diet reconstruction using mixing models. Nevertheless, the results reported here revealed that the stable isotope ratios in squamosal and rib bone capture

much of the variability observed in the epidermis and hence are useful to make inferences on the trophic ecology of green turtles.

Acknowledgements We want to thank Alexander Gaos, Summer Martin, Camryn Allen, and Shandell Brunson (deceased) from NOAA Fisheries, Hawaii and Garrett E. Lemons, and Calandra Turner Tomaszewicz from NOAA Fisheries, La Jolla and Marc Rice from the Hawaii Preparatory Academy. We also want to thank Cathy Gewecke from the Department of Land and Natural Resources, Oahu, Hawaii, Alan Giraldo from Grupo de Ecología de la Universidad del Valle in Colombia and Benjamin A. Harlow from the Stable Isotope Core Laboratory, WSU, for their invaluable advice and support.

Author contributions All authors contributed to the study's conception and design. AV and LC: performed material preparation, data collection, and analysis. Samples were collected by AV, LC, and GB. The first draft of the manuscript was written by AV, LC, and JS. All authors commented on previous versions, read and approved the final manuscript.

Funding Open Access funding provided thanks to the CRUE-CSIC agreement with Springer Nature. This work was partly supported by Fundació Bosch i Gimpera, Barcelona, Spain (project: 309765).

Data availability The datasets analyzed during the current study are available in this article and the supplementary information.

Declarations

Conflict of interest None of the authors have conflicts of interest in this study. All activities performed to collect sea turtle samples were permitted by National Oceanic and Atmospheric Administration (NOAA) and National Marine Fisheries Service (NMFS) permits: 1581, 1581e01, 15685, 10027e05, 15661e01, 17022, and 21260; U.S. Fish and Wildlife Service (USFWS) permits: TE-70288A-3, 12533e12008, and 12533e13001; and State of Hawai'i permit 2013e32 and 2023-02. Sampling at Kaloko-Honokōhau National Historical Park was conducted under special activity permit No. 2019-52 from the Department of Land and Natural Resources, Hawaii, and permit KAHO-2018-SCI-00 for Scientific Research and Collecting Permit by the U.S. National Park Service (NPS). All guidelines for sampling have been followed.

Open Access This article is licensed under a Creative Commons Attribution 4.0 International License, which permits use, sharing, adaptation, distribution and reproduction in any medium or format, as long as you give appropriate credit to the original author(s) and the source, provide a link to the Creative Commons licence, and indicate if changes were made. The images or other third party material in this article are included in the article's Creative Commons licence, unless indicated otherwise in a credit line to the material. If material is not included in the article's Creative Commons licence and your intended use is not permitted by statutory regulation or exceeds the permitted use, you will need to obtain permission directly from the copyright holder. To view a copy of this licence, visit <http://creativecommons.org/licenses/by/4.0/>.

References

- Allen J (1998) Mangroves as alien species: the case of Hawaii. *Glob Ecol Biogeogr* 7:61–71. <https://doi.org/10.1111/j.1466-8238.1998.00272.x>
- Amarocho DF, Reina RD (2007) Feeding ecology of the East Pacific green sea turtle *Chelonia mydas agassizii* at Gorgona National Park Colombia. *Endanger Species Res* 3:43–51
- Arencibia A, Rivero M, De Miguel I, Contreras S, Cabrero A, Orós J (2006) Computed tomographic anatomy of the head of the loggerhead sea turtle (*Caretta caretta*). *Res Vet Sci* 81:165–169. <https://doi.org/10.1016/j.rvsc.2005.12.009>
- Arthur KE, Balazs GH (2008) A comparison of immature green turtle (*Chelonia mydas*) diets among seven sites in the main Hawaiian Islands. *Pac Sci* 62:205–218. [https://doi.org/10.2984/1534-6188\(2008\)62\[205:ACOIGT\]2.0.CO;2](https://doi.org/10.2984/1534-6188(2008)62[205:ACOIGT]2.0.CO;2)
- Balazs GH (1976) Green turtle migrations in the Hawaiian Archipelago. *Biol Conserv* 9:125–140. [https://doi.org/10.1016/0006-3207\(76\)90045-8](https://doi.org/10.1016/0006-3207(76)90045-8)
- Balazs GH, Chaloupka M (2004) Spatial and temporal variability in somatic growth of green sea turtles (*Chelonia mydas*) resident in the Hawaiian Archipelago. *Mar Biol* 145:1043–1059. <https://doi.org/10.1007/s00227-004-1387-6>
- Bas M, Cardona L (2018) Effects of skeletal element identity, delipidation and demineralization on the analysis of stable isotope ratios of C and N in fish bone. *J Fish Biol* 92:420–437. <https://doi.org/10.1111/jfb.13521>
- Bas M, Salemm M, Green EJ, Santiago F, Speller C, Álvarez M, Briz i Godino I, Cardona L (2020) Predicting habitat use by the Argentine hake *Merluccius hubbsi* in a warmer world: inferences from the Middle Holocene. *Oecologia* 193:461–474. <https://doi.org/10.1007/s00442-020-04667-z>
- Bearhop S, Waldron S, Votier SC, Furness RW (2002) Factors that influence assimilation rates and fractionation of nitrogen and carbon stable isotopes in avian blood and feathers. *Physiol Biochem Zool* 75:451–458. <https://doi.org/10.1086/342800>
- Bjorndal KA, Bolten AB, Dellinger T, Delgado C, Martins HR (2003) Compensatory growth in oceanic loggerhead sea turtles: response to a stochastic environment. *Ecology* 84:1237–1249. [https://doi.org/10.1890/0012-9658\(2003\)084\[1237:CGIOLS\]2.0.CO;2](https://doi.org/10.1890/0012-9658(2003)084[1237:CGIOLS]2.0.CO;2)
- Braje TJ, Rick TC, Szpak P, Newsome SD, McCain JM, Elliott Smith EA, Glassow M, Hamilton SL (2017) Historical ecology and the conservation of large, hermaphroditic fishes in Pacific Coast kelp forest ecosystems. *Sci Adv* 3:e1601759. <https://doi.org/10.1126/sciadv.1601759>
- Brenna JT, Corso TN, Tobias HJ, Caimi RJ (1997) High-precision continuous-flow isotope ratio mass spectrometry. *Mass Spectrom Rev* 16:227–258. [https://doi.org/10.1002/\(SICI\)1098-2787\(1997\)16:5%3C227::AID-MAS1%3E3.0.CO;2-J](https://doi.org/10.1002/(SICI)1098-2787(1997)16:5%3C227::AID-MAS1%3E3.0.CO;2-J)
- Cardona L, Aguilar A, Pazos L (2009) Delayed ontogenic dietary shift and high levels of omnivory in green turtles (*Chelonia mydas*) from the NW coast of Africa. *Mar Biol* 156:1487–1495. <https://doi.org/10.1007/s00227-009-1188-z>
- Cardona L, Campos P, Levy Y, Demetropoulos A, Margaritoulis D (2010) Asynchrony between dietary and nutritional shifts during the ontogeny of green turtles (*Chelonia mydas*) in the Mediterranean. *J Exp Mar Biol Ecol* 393:83–89. <https://doi.org/10.1016/j.jembe.2010.07.004>
- Cardona L, Campos P, Velásquez-Vacca A (2020) Contribution of green turtles *Chelonia mydas* to total herbivore biomass in shallow tropical reefs of oceanic islands. *PLoS ONE* 15:e0228548. <https://doi.org/10.1371/journal.pone.0228548>
- Castanet J, Smirina E (1990) Introduction to the skeletochronological method in amphibians and reptiles. *Ann Sci Nat Zool* 11:191–196
- Cheroske AG, Williams SL, Carpenter RC (2000) Effects of physical and biological disturbances on algal turfs in Kāne'ohe Bay, Hawaii *J Exp Mar Biol Ecol* 248:1–34. [https://doi.org/10.1016/S0022-0981\(00\)00153-2](https://doi.org/10.1016/S0022-0981(00)00153-2)
- Choy ES, Giraldo C, Rosenberg B, Roth JD, Ehrman AD, Majewski A, Swanson H, Power M, Reist JD, Loseto LL (2020) Variation in the

- diet of beluga whales in response to changes in prey availability: insights on changes in the Beaufort Sea ecosystem. *Mar Ecol Prog Ser* 647:195–210. <https://doi.org/10.3354/meps13413>
- Clark CT, Horstmann L, Misarti N (2017) Quantifying variability in stable carbon and nitrogen isotope ratios within the skeletons of marine mammals of the suborder Caniformia. *J Archaeol Sci Rep* 15:393–400. <https://doi.org/10.1016/j.jasrep.2017.09.007>
- Connolly RM, Schlacher TA (2013) Sample acidification significantly alters stable isotope ratios of sulfur in aquatic plants and animals. *Mar Ecol Prog Ser* 493:1–8. <https://doi.org/10.3354/meps10560>
- Connolly RM, Guest MA, Melville AJ, Oakes JM (2004) Sulfur stable isotopes separate producers in marine food-web analysis. *Oecologia* 138:161–167. <https://doi.org/10.1007/s00442-003-1415-0>
- DeNiro MJ, Epstein S (1978) Influence of diet on the distribution of carbon isotopes in animals. *Geochim Cosmochim Acta* 42:495–506. [https://doi.org/10.1016/0016-7037\(78\)90199-0](https://doi.org/10.1016/0016-7037(78)90199-0)
- Drupp P, De Carlo EH, Mackenzie FT, Bienfang P, Sabine CL (2011) Nutrient inputs, phytoplankton response, and CO₂ variations in a semi-enclosed subtropical embayment, Kāneʻohe Bay, Hawaii. *Aquat Geochem* 17:473–498. <https://doi.org/10.1007/s10498-010-9115-y>
- Ehrlich H (2010) *Biological materials of marine origin*. Springer, Dordrecht
- Esteban N, Mortimer JA, Stokes HJ, Laloë J-O, Unsworth RK, Hays GC (2020) A global review of green turtle diet: sea surface temperature as a potential driver of omnivory levels. *Mar Biol* 167:1–17. <https://doi.org/10.1007/s00227-020-03786-8>
- Fahy GE, Deter C, Pitfield R, Miszkiewicz JJ, Mahoney P (2017) Bone deep: variation in stable isotope ratios and histomorphometric measurements of bone remodelling within adult humans. *J Archaeol Sci* 87:10–16. <https://doi.org/10.1016/j.jas.2017.09.009>
- Fleming AH, Clark CT, Calambokidis J, Barlow J (2016) Humpback whale diets respond to variance in ocean climate and ecosystem conditions in the California Current. *Glob Chang Biol* 22:1214–1224. <https://doi.org/10.1111/gcb.13171>
- Folch J, Lees M, Sloane Stanley GH (1957) A simple method for the isolation and purification of total lipids from animal tissues. *J Biol Chem* 226:497–509. [https://doi.org/10.1016/S0021-9258\(18\)64849-5](https://doi.org/10.1016/S0021-9258(18)64849-5)
- Friedlander A, Aeby G, Brainard R, Brown E, Chaston K, Clark A, McGowan P, Montgomery T, Walsh W, Williams I (2008) The state of coral reef ecosystems of the main Hawaiian Islands. *State Coral Reef Ecosyst United States Pacific Freely Assoc States* 17:222–269
- Fry B, Smith TJ (2002) Stable isotope studies of red mangroves and filter feeders from the Shark River estuary. *Florida Bull Mar Sci* 70:871–890
- Fry B, Silva SR, Kendall C, Anderson RK (2002) Oxygen isotope corrections for online $\delta^{34}\text{S}$ analysis. *Rapid Commun Mass Spectrom* 16:854–858. <https://doi.org/10.1002/rcm.651>
- Gillis AJ, Ceriani SA, Seminoff JA, Fuentes MM (2018) Foraging ecology and diet selection of juvenile green turtles in the Bahamas: insights from stable isotope analysis and prey mapping. *Mar Ecol Prog Ser* 599:225–238. <https://doi.org/10.3354/meps12635>
- González Carman V, Botto F, Gaitán E, Albareda D, Campagna C, Mianzan H (2014) A jellyfish diet for the herbivorous green turtle *Chelonia mydas* in the temperate SW Atlantic. *Mar Biol* 161:339–349. <https://doi.org/10.1007/s00227-013-2339-9>
- Hanson NN, Wurster CM, Bird MI, Reid K, Boyd IL (2009) Intrinsic and extrinsic forcing in life histories: patterns of growth and stable isotopes in male Antarctic fur seal teeth. *Mar Ecol Prog Ser* 388:263–272. <https://doi.org/10.3354/meps08158>
- Jones TT, Seminoff J (2013) Feeding biology: advances from field-based observations, physiological studies, and molecular techniques. *Biol Sea Turtles* 3:211–247. <https://doi.org/10.1201/b13895>
- Jones ME, Werneburg I, Curtis N, Penrose R, O'Higgins P, Fagan MJ, Evans SE (2012) The head and neck anatomy of sea turtles (Cryptodira: Chelonioidae) and skull shape in Testudines. *PLoS ONE* 7:e47852. <https://doi.org/10.1371/journal.pone.0047852>
- Koch PL, Michener R, Lajtha K (2007) Isotopic study of the biology of modern and fossil vertebrates. *Stable Isot Ecol Environ Sci* 2:99–154. <https://doi.org/10.1002/9780470691854.ch5>
- Layman CA, Araujo MS, Boucek R, Hammerschlag-Peyer CM, Harrison E, Jud ZR, Matich P, Rosenblatt AE, Vaudo JJ, Yeager LA (2012) Applying stable isotopes to examine food-web structure: an overview of analytical tools. *Biol Rev* 87:545–562. <https://doi.org/10.1111/j.1469-185X.2011.00208.x>
- Lazarus BS, Velasco-Hogan A, Gómez-del Río T, Meyers MA, Jasiuk I (2020) A review of impact resistant biological and bioinspired materials and structures. *J Mater Res Technol J Mater Res Technol* 9:15705–15738. <https://doi.org/10.1016/j.jmrt.2020.10.062>
- Lemons G, Lewison R, Komoroske L, Gaos A, Lai C-T, Dutton P, Eguchi T, LeRoux R, Seminoff JA (2011) Trophic ecology of green sea turtles in a highly urbanized bay: insights from stable isotopes and mixing models. *J Exp Mar Biol Ecol* 405:25–32. <https://doi.org/10.1016/j.jembe.2011.05.012>
- Lesser MP (2021) Eutrophication on coral reefs: what is the evidence for phase shifts, nutrient limitation and coral bleaching. *BioScience* 71:1216–1233. <https://doi.org/10.1093/biosci/biab101>
- Limpus CJ, Limpus DJ (2000) Mangroves in the diet of *Chelonia mydas* in Queensland, Australia. *Mar Turt Newsl* 89:13–15
- McCutchan JH Jr, Lewis WM Jr, Kendall C, McGrath CC (2003) Variation in trophic shift for stable isotope ratios of carbon, nitrogen, and sulfur. *Oikos* 102:378–390. <https://doi.org/10.1034/j.1600-0706.2003.12098.x>
- McDermid KJ, Stuercke B (2003) Nutritional composition of edible Hawaiian seaweeds. *J Appl Phycol* 15:513–524. <https://doi.org/10.1023/B:JAPH.0000004345.31686.7f>
- McDermid KJ, Gregoritz MC, Freshwater DW (2002) A new record of a second seagrass species from the Hawaiian archipelago: *Halophila decipiens* Ostenfeld. *Aquat Bot* 74:257–262. [https://doi.org/10.1016/S0304-3770\(02\)00081-5](https://doi.org/10.1016/S0304-3770(02)00081-5)
- McDermid KJ, Stuercke B, Balazs GH (2007) Nutritional composition of marine plants in the diet of the green sea turtle (*Chelonia mydas*) in the Hawaiian Islands. *Bull Mar Sci* 81:55–71
- McDermid KJ, Lefebvre JA, Balazs GH (2015) Nonnative seashore paspalum, *Paspalum vaginatum* (Poaceae), consumed by Hawaiian green sea turtles (*Chelonia mydas*): Evidence for nutritional benefits. *Pac Sci* 69:48–57. <https://doi.org/10.2984/69.1.3>
- McDermid K, Jha R, Rice M, Balazs G (2018) Of turtles and trees: nutritional analysis. *Micronesica* 2018–02:1–11
- Medeiros L, da Silveira MD, Petitet R, Bugoni L (2015) Effects of lipid extraction on the isotopic values of sea turtle bone collagen. *Aquat Biol* 23:191–199. <https://doi.org/10.3354/ab00628>
- Nagaoka SM, Martins AS, Dos Santos RG, Tognella MMP, de Oliveira Filho EC, Seminoff JA (2012) Diet of juvenile green turtles (*Chelonia mydas*) associating with artisanal fishing traps in a subtropical estuary in Brazil. *Mar Biol* 159:573–581. <https://doi.org/10.1007/s00227-011-1836-y>
- Pagès Barceló L, Seminoff JA, Vander Zanden HB, Jones TT, Bjørndal KA, Bolten AB, Mustin W, Busquets-Vass G, Newsome SD (2021) Hydrogen isotope assimilation and discrimination in green turtles. *J Exp Biol* 224:jeb231431. <https://doi.org/10.1242/jeb.231431>
- Parker DM, Dutton PH, Balazs GH (2011) Oceanic diet and distribution of haplotypes for the green turtle, *Chelonia mydas*, in the Central North Pacific. *Pac Sci* 65:419–431. <https://doi.org/10.2984/65.4.419>
- Phillips DL, Inger R, Bearhop S, Jackson AL, Moore JW, Parnell AC, Semmens BX, Ward EJ (2014) Best practices for use of

- stable isotope mixing models in food-web studies. *Can J Zool* 92:823–835. <https://doi.org/10.1139/cjz-2014-0127>
- Piacenza SE, Balazs GH, Hargrove SK, Richards PM, Heppell SS (2016) Trends and variability in demographic indicators of a recovering population of green sea turtles *Chelonia mydas*. *Endanger Species Res* 31:103–117. <https://doi.org/10.3354/esr00753>
- Post DM (2002) Using stable isotopes to estimate trophic position: models, methods, and assumptions. *Ecology* 83:703–718
- Qi H, Coplen TB (2003) Evaluation of the $^{34}\text{S}/^{32}\text{S}$ ratio of Soufre de Lacq elemental sulfur isotopic reference material by continuous flow isotope-ratio mass spectrometry. *Chem Geol* 199:183–187. [https://doi.org/10.1016/S0009-2541\(03\)00075-5](https://doi.org/10.1016/S0009-2541(03)00075-5)
- R Core Team (2021) R: a language and environment for statistical computing. R Foundation for Statistical Computing, Vienna, Austria. <https://www.R-project.org/>
- Reich KJ, Bjorndal KA, Bolten AB (2007) The ‘lost years’ of green turtles: using stable isotopes to study cryptic lifestages. *Biol Lett* 3:712–714
- Reich KJ, Bjorndal KA, Martínez del Río C (2008) Effects of growth and tissue type on the kinetics of ^{13}C and ^{15}N incorporation in a rapidly growing ectotherm. *Oecologia* 155:651–663. <https://doi.org/10.1007/s00442-007-0949-y>
- Rodrigues C, Brunner M, Steiman S, Bowen GJ, Nogueira JM, Gautz L, Prohaska T, Máguas C (2011) Isotopes as tracers of the Hawaiian coffee-producing regions. *J Agric Food Chem* 59:10239–10246. <https://doi.org/10.1021/jf200788p>
- Russell DJ, Balazs GH (2009) Dietary shifts by green turtles (*Chelonia mydas*) in the Kāne’ohe bay region of the Hawaiian islands: a 28-Year Study. *Pac Sci* 63:181–193. <https://doi.org/10.2984/049.063.0202>
- Russell DJ, Balazs GH (2015) Increased use of non-native algae species in the diet of the green turtle (*Chelonia mydas*) in a primary pasture ecosystem in Hawaii. *Aquat Ecosyst Health Manag* 18:342–346. <https://doi.org/10.1080/14634988.2015.1027140>
- Russell DJ, Balazs GH, Phillips RC, Kam AK (2003) Discovery of the sea grass *Halophila decipiens* (Hydrocharitaceae) in the diet of the Hawaiian green turtle, *Chelonia mydas*. *Pac Sci* 57:393–397. <https://doi.org/10.1353/psc.2003.0034>
- Russell DJ, Hargrove S, Balazs GH (2011) Marine sponges, other animal food, and nonfood items found in digestive tracts of the herbivorous marine turtle *Chelonia mydas* in Hawai’i. *Pac Sci* 65:375–381. <https://doi.org/10.2984/65.3.375>
- Santrock J, Studley SA, Hayes J (1985) Isotopic analyses based on the mass spectra of carbon dioxide. *Anal Chem* 57:1444–1448. <https://doi.org/10.1021/ac00284a060>
- Seminoff JA, Jones TT, Marshall GJ (2006) Underwater behaviour of green turtles monitored with video-time-depth recorders: what’s missing from dive profiles? *Mar Ecol Prog Ser* 322:269–280. <https://doi.org/10.3354/meps322269>
- Seminoff JA, Allen CD, Balazs GH, Dutton PH, Eguchi T, Haas H, Hargrove SA, Jensen M, Klemm DL, Lauritsen AM, MacPherson SL, Opat P, Possardt EE, Pultz S, Seney EE, Van Houtan KS, Waples RS (2015) Status review of the green turtle (*Chelonia mydas*) under the Endangered Species Act. US Department of Commerce, National Oceanic and Atmospheric Administration, National Marine Fisheries Service NOAA technical memorandum, National Marine Fisheries Service
- Skedros JG, Knight AN, Clark GC, Crowder CM, Dominguez VM, Qiu S, Mulhern DM, Donahue SW, Busse B, Hulsey BI (2013) Scaling of Haversian canal surface area to secondary osteon bone volume in ribs and limb bones. *Am J Phys Anthropol* 151:230–244. <https://doi.org/10.1002/ajpa.22270>
- Smith KJ, Sparks JP, Timmons ZL, Peterson MJ (2020) Cetacean skeletons demonstrate ecologically relevant variation in intraskeletal stable isotopic values. *Front Mar Sci* 7:388. <https://doi.org/10.3389/fmars.2020.00388>
- Snover ML, Hohn AA, Goshe LR, Balazs GH (2011) Validation of annual skeletal marks in green sea turtles *Chelonia mydas* using tetracycline labeling. *Aquat Biol* 12:197–204. <https://doi.org/10.3354/ab00337>
- Standora E, Morreale S, Ruiz G, Spotila J (1982) Sex determination in green turtle (*Chelonia mydas*) hatchlings can be influenced by egg position within the nest. *Bull Ecol Soc Am* 63:83–84
- Stock BC, Jackson AL, Ward EJ, Parnell AC, Phillips DL, Semmens BX (2018) Analyzing mixing systems using a new generation of Bayesian tracer mixing models. *PeerJ* 6:e5096. <https://doi.org/10.7717/peerj.5096>
- Swierts T, Vermeij MJ (2016) Competitive interactions between corals and turf algae depend on coral colony form. *PeerJ* 4:e1984. <https://doi.org/10.7717/peerj.1984>
- Tennekes M (2018) tmap: thematic maps in R. *J Stat Softw* 84:1–39. <https://doi.org/10.18637/jss.v084.i06>
- Turner Tomaszewicz CN, Seminoff JA, Ramirez MD, Kurle CM (2015) Effects of demineralization on the stable isotope analysis of bone samples. *Rapid Commun Mass Spectrom* 29:1879–1888. <https://doi.org/10.1002/rcm.7295>
- Turner Tomaszewicz CN, Seminoff JA, Price M, Kurle CM (2017) Stable isotope discrimination factors and between-tissue isotope comparisons for bone and skin from captive and wild green sea turtles (*Chelonia mydas*). *Rapid Commun Mass Spectrom* 31:1903–1914. <https://doi.org/10.1002/rcm.7974>
- Turner Tomaszewicz CN, Seminoff JA, Avens L, Goshe LR, Rguez-Baron JM, Peckham SH, Kurle CM (2018) Expanding the coastal forager paradigm: long-term pelagic habitat use by green turtles *Chelonia mydas* in the eastern Pacific Ocean. *Mar Ecol Prog Ser* 587:217–234. <https://doi.org/10.3354/meps12372>
- Turner Tomaszewicz CN, Avens L, LaCasella EL, Eguchi T, Dutton PH, LeRoux RA, Seminoff JA (2022a) Mixed-stock aging analysis reveals variable sea turtle maturity rates in a recovering population. *J Wildl Manag* 86:e22217. <https://doi.org/10.1002/jwmg.22217>
- Turner Tomaszewicz CN, Avens L, Seminoff JA, Limpus CJ, FitzSimmons NN, Guinea ML, Pendoley KL, Whittock PA, Vitenbergs A, Whiting SD (2022b) Age-specific growth and maturity estimates for the flatback sea turtle (*Natator depressus*) by skeletochronology. *PLoS ONE* 17:e0271048. <https://doi.org/10.1371/journal.pone.0271048>
- Wabnitz CC, Balazs G, Beavers S, Bjorndal KA, Bolten AB, Christensen V, Hargrove S, Pauly D (2010) Ecosystem structure and processes at Kaloko Honokōhau, focusing on the role of herbivores, including the green sea turtle *Chelonia mydas*, in reef resilience. *Mar Ecol Prog Ser* 420:27–44. <https://doi.org/10.3354/meps08846>
- Wallace BP, DiMatteo AD, Hurley BJ, Finkbeiner EM, Bolten AB, Chaloupka MY, Hutchinson BJ, Abreu-Grobois FA, Amoroch D, Bjorndal KA (2010) Regional management units for marine turtles: a novel framework for prioritizing conservation and research across multiple scales. *PLoS ONE* 5:e15465. <https://doi.org/10.1371/journal.pone.0015465>
- Williams I, Walsh W, Schroeder R, Friedlander A, Richards B, Stamoulis K (2008) Assessing the importance of fishing impacts on Hawaiian coral reef assemblages along regional-scale human population gradients. *Environ Conserv* 35:261–272. <https://doi.org/10.1017/S0376892908004876>
- Zenteno L, Borella F, Otero JG, Piana E, Belardi JB, Borrero LA, Saporiti F, Cardona L, Crespo E (2015a) Shifting niches of marine predators due to human exploitation: the diet of the South American sea lion (*Otaria flavescens*) since the late Holocene as a case study. *Paleobiology* 41:387–401. <https://doi.org/10.1017/pab.2015.9>

Zenteno L, Crespo E, Vales D, Silva L, Saporiti F, Oliveira LR, Secchi ER, Drago M, Aguilar A, Cardona L (2015b) Dietary consistency of male South American sea lions (*Otaria flavescens*) in southern Brazil during three decades inferred from stable isotope analysis. *Mar Biol* 162:275–289. <https://doi.org/10.1007/s00227-014-2597-1>

Publisher's Note Springer Nature remains neutral with regard to jurisdictional claims in published maps and institutional affiliations.